ORGANOMETALLICS

Article

Cite This: *Organometallics* XXXX, XXX, XXX−XXX

pubs.acs.org/Organometallics

# Metalation and Methyl Group Migration in 21-, 22-, and 23-Methylcarbaporphyrins: Synthesis and Characterization of Palladium(II), Rhodium(I), and Rhodium(III) Derivatives

Alissa N. Latham, Gregory M. Ferrence, and Timothy D. Lash*

Department of Chemistry, Illinois State University, Normal, Illinois 61790-4160, United States

Supporting Information

**ABSTRACT:** A rational synthesis of 23-methylcarbaporphyrin has been developed. 3,4-Diethyl-1-methylpyrrole reacted with acetoxymethylpyrrole under acidic conditions to give *N*-methyltripyrrane, and following cleavage of the ester protective groups, the tripyrrolic intermediate condensed with an indene dialdehyde in the presence of trifluoroacetic acid to afford the required *N*-methylcarbaporphyrin. Reaction with palladium(II) acetate in refluxing acetonitrile for short time periods gave a 23-methyl palladium(II) complex but prolonged reaction times afforded a rearranged 21-methyl product. The 23-methyl complex can be isolated but gradually converts into the 21-methyl derivative even in the solid state. 21-Methyl- and 22-methylcarbaporphyrins reacted with $[Rh(CO)_2Cl]_2$ to give rhodium(I) complexes. However, when the 23-methylcarbaporphyrin was reacted under the same conditions, a rhodium(III) derivative was isolated. This complex incorporates a bridging methylene unit between the Rh(III) and the 21-carbon and must therefore be formed by a methyl group migration−cyclization process.

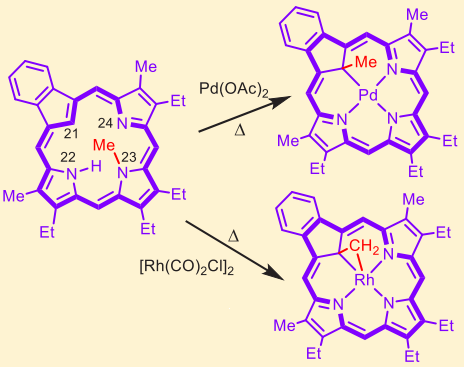




## INTRODUCTION

The porphyrins are among the most versatile of ligands and form complexes with virtually every metal or metalloid in the periodic table.[1] This versatility is due in part to their NNNN coordination core which can facilitate square planar complexation, but they also retain sufficient flexibility to allow for other coordination motifs.[1] Core-modified porphyrins, where one or more of the internal nitrogens have been replaced by other elements such as O, S, Se, Te, or P, also exhibit interesting coordination chemistry,[2] although these ligands are far less versatile. Carbaporphyrins (e.g., **1** and **2**) and related systems,[3] such as N-confused porphyrins **3**,[4] azuliporphyrins **4**,[5] and benziporphyrins **5**,[6] have carbons in place of one or more of the core nitrogen atoms (Figure 1). Although these macrocycles can only coordinate with a smaller number of metal cations compared to porphyrins, they readily form stable organometallic derivatives with a number of late transition metal ions.[7] Azuliporphyrins generally act as dianionic ligands, forming organometallic complexes with Ni(II),[8] Pd(II),[8] Pt(II),[8] and Ru(II).[9] Rh(III) and Ir(III) azuliporphyrins have also been reported,[10,11] but these possess additional axial carbon ligands. Benziporphyrins are also dianionic ligands,[12] whereas N-confused porphyrins can act as both dianionic or trianionic ligands.[13] True carbaporphyrins such as **1** and **2** are trianionic ligands and have been shown to form Ag(III),[14−16] Au(III),[15] Rh(III),[17] and Ir(III)[17] derivatives. However, the coordination chemistry can be altered by replacing one of the remaining nitrogens with oxygen, sulfur, or selenium. For instance, 23-oxa-, 23-thia- and 23-selena-21-carbaporphyrins **6a−c** reacted with palladium(II) acetate in refluxing acetonitrile to give palladium(II) complexes **7a−c** (Scheme 1).[18] Nickel(II) acetate also reacted with **6a** or **6b** to afford the related nickel(II) derivatives **8a,b**, but when the reaction was carried out in the presence of air, oxy-heterocarbaporphyrins **9a,b** were isolated instead.[18] Reports of related organometallic complexes such as **10**[19] and **11**[20] have also appeared (Figure 2).

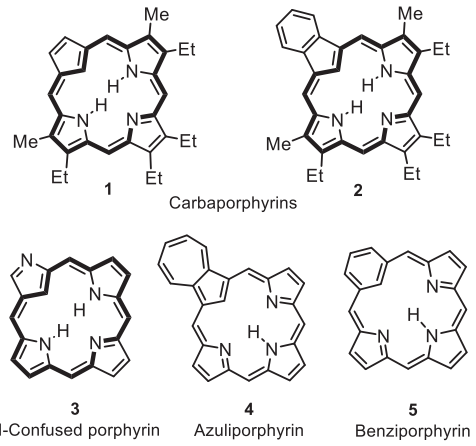


**Figure 1.** Selected examples of carbaporphyrinoid systems.

In an attempt to alter the coordination chemistry of regular carbaporphyrins, **2** was reacted with methyl or ethyl iodide and

**Received:** November 28, 2018




DOI: 10.1021/acs.organomet.8b00863
*Organometallics* XXXX, XXX, XXX−XXX

**Scheme 1. Metalation and Oxidation of 23-Heterocarbaporphyrins**[18]

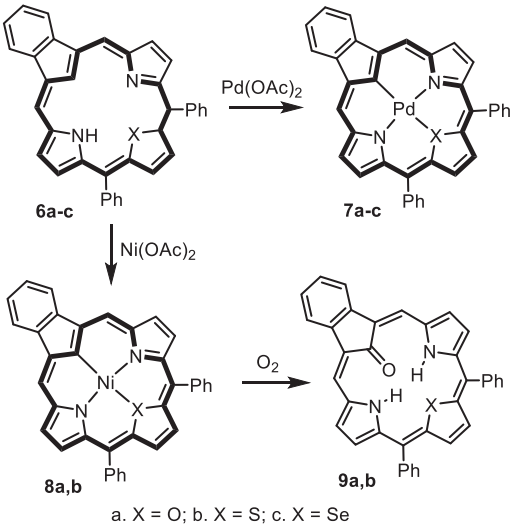


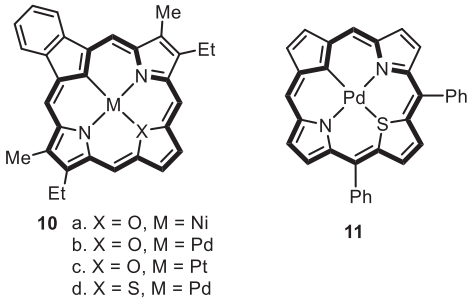


**Figure 2.** Examples of metalated heterocarbaporphyrins.

potassium carbonate in refluxing acetone.[21] The major products resulting from these reactions were 22-alkylcarbaporphyrins **12**, although C-alkylated byproducts **13** were also observed (Scheme 2). Having replaced one of the inner hydrogens with an alkyl group in **12a,b**, it was anticipated that the porphyrin analogues would now act as dianionic ligands. Reaction of **12a** or **12b** with $Pd(OAc)_2$ in refluxing acetonitrile

**Scheme 2. Alkylation and Metalation of a Carbaporphyrin**[21]

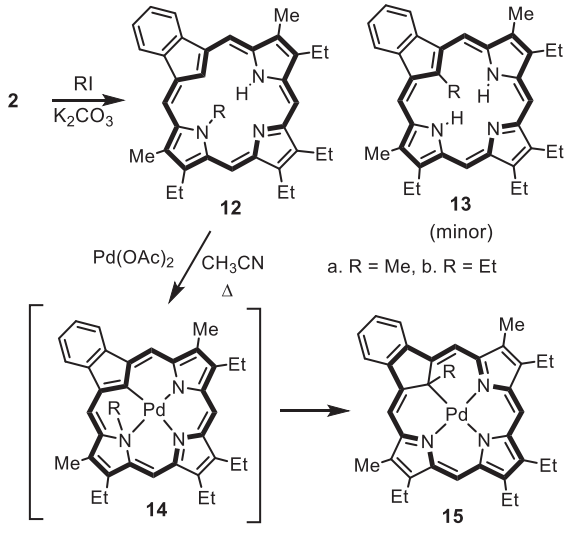


initially gave Pd(II) complexes **14a** or **14b**, but these rapidly rearranged to give the C-alkyl complexes **15**. When the reaction was carried out for 5 min, *N*-alkyl derivatives **14a,b** were the major products, but after 30 min, virtually all of the material had been converted into **15a,b**.[21] Attempts to purify **14a** or **14b** by column chromatography were unsuccessful as partial conversion to **15a,b** occurred even at room temperature. The mechanism for this rearrangement is not currently known. It was suggested that a [3,3]sigmatropic rearrangement could be involved or that a transient palladium–alkyl complex was responsible for the transference.[21] Similar rearrangements were subsequently observed for carbaporphyrins without fused benzo units[22] and with naphthocarba[2,3-*b*]porphyrins.[23] Palladium(II)-catalyzed rearrangements of *p*-benziporphyrins to give related palladium(II) carbaporphyrins have been reported,[24] and palladium-mediated rearrangements of vacataporphyrin[25] and some expanded porphyrin systems have been noted.[26] Therefore, reactions of this type appear to have considerable significance and warrant further investigation. In order to further probe this chemistry, the synthesis of a 23-methylcarbaporphyrin **16** was carried out, and the formation of palladium and rhodium derivatives was investigated.

## RESULTS AND DISCUSSION

**Methyl Group Migration in Palladium(II) Carbaporphyrins.** Alkylation of carbaporphyrin **2** gave 22-alkyl (major) and 21-alkyl (minor) products **12** and **13**, respectively, but 23-alkyl derivatives were not observed.[21] Investigations into the metalation of 23-methylcarbaporphyrin **16** were of great potential interest because this system could not undergo a simple [3,3]sigmatropic rearrangement to give a C-methyl palladium complex. Therefore, metalation studies on **16** would provide insights into the alkyl group migrations previously observed for 22-alkylcarbaporphyrins. A rational synthesis of **16** was developed using the "3 + 1" version of the MacDonald condensation (Scheme 3).[27] Ethyl 3,4-diethylpyrrole-2-carboxylate (**17a**) was prepared by reacting 3-acetoxy-4-nitrohexane with ethyl isocyanoacetate and 2 equiv of 1,8-diazabicyclo[5.4.0]undec-7-ene (DBU) in THF–isopropyl alcohol (Barton-Zard condensation). The product was isolated

**Scheme 3. MacDonald-Type "3 + 1" Synthesis of a 23-Methylcarbaporphyrin**

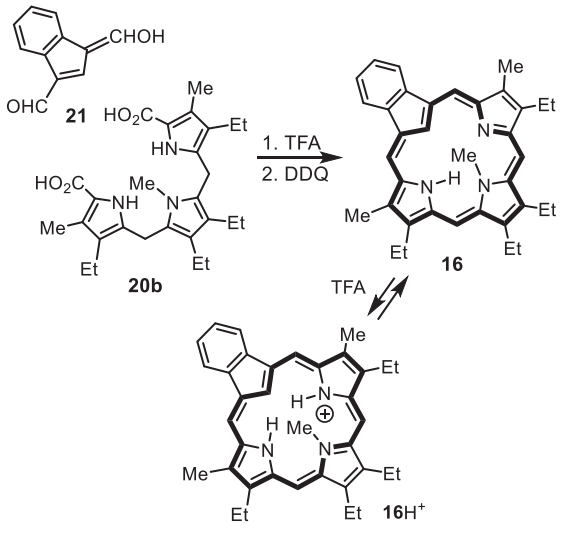




DOI: 10.1021/acs.organomet.8b00863
*Organometallics* XXXX, XXX, XXX–XXX

in 70% yield, but the NMR spectrum showed that **17a** was contaminated with approximately 3% of the corresponding isopropyl ester. As the ester group was saponified at a later stage in the synthesis, **17a** was used in this form. Alkylation of **17a** with methyl iodide and KOH in DMSO afforded the corresponding *N*-methyl derivative **17b** (Scheme 4), and

**Scheme 4. Synthesis of a *N*-Methyltripyrrane**

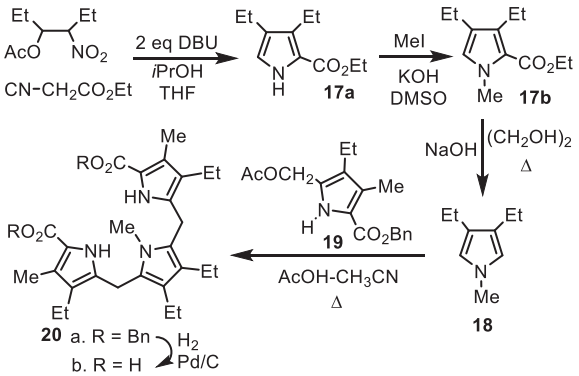


subsequent saponification and decarboxylation with sodium hydroxide in ethylene glycol at >180 °C generated 3,4-diethyl-1-methylpyrrole (**18**). Pyrrole **18** had previously been prepared from 1,2-dimethylhydrazine using a variation on the Fischer indole synthesis.[28] Tripyrranes can be prepared by condensing $\alpha,\alpha'$-diunsubstituted pyrroles with 2 equiv of an acetoxymethylpyrrole (e.g., **19**) in the presence of an acid catalyst.[29] However, attempts to react **18** with **19** in the presence of Montmorillonite clay[30] gave poor results, and reactions with acetic acid in ethanol or other alcohol solvents[31] also gave low yields of the desired tripyrrolic product **20a**. Superior results were obtained by refluxing the reactants with acetic acid in acetonitrile under nitrogen. Unlike N-unsubstituted tripyrranes, tripyrrane **20a** failed to precipitate from solution and had to be purified by column chromatography. Some tripyrranes decompose during chromatography, but this problem did not arise in this case, and **20a** could be isolated as an oil that solidified in the freezer. Hydrogenolysis of the benzyl ester protective groups over 10% palladium charcoal gave the related dicarboxylic acid **20b**.

*N*-Alkyl tripyrranes had not previously been applied to the preparation of porphyrinoid products. However, "2 + 2" MacDonald condensation of a *N*-methyldipyrrylmethane with a dipyrrylmethane dialdehyde had been used to synthesize a *N*-methylporphyrin,[32] and related porphyrins were prepared from *a,c*-biladiene intermediates.[33] The presence of an internal substituent might sterically inhibit cyclization, and given the instability of tripyrranes under the acidic conditions used to carry out these reactions, there was a possibility that decomposition would ensue. Fortunately, when **20b** was reacted with indene dialdehyde **21**[34] in the presence of TFA, followed by oxidation with DDQ, the targeted 23-methylcarbaporphyrin **16** was generated in 32% yield. Fairly concentrated conditions were used (<20 mL of dichloromethane for every 100 mg of tripyrrane), but no improvement in yield was observed under more dilute conditions. The carbaporphyrin was purified by column chromatography, followed by recrystallization from chloroform–methanol. The N-substituted carbaporphyrin retains fully aromatic characteristics, and the proton NMR spectrum in $CDCl_3$ showed the *meso*-protons as two downfield singlets at 9.67 and 10.02 ppm. The internal methyl group is strongly shifted upfield to give a 3H singlet at −4.21 ppm, whereas the internal CH afforded a resonance at −4.86 ppm, and the NH appears as a broad peak between 0 and −1 ppm. Carbaporphyrin **16** gave a UV–vis spectrum (Figure 3) that was typical of an aromatic

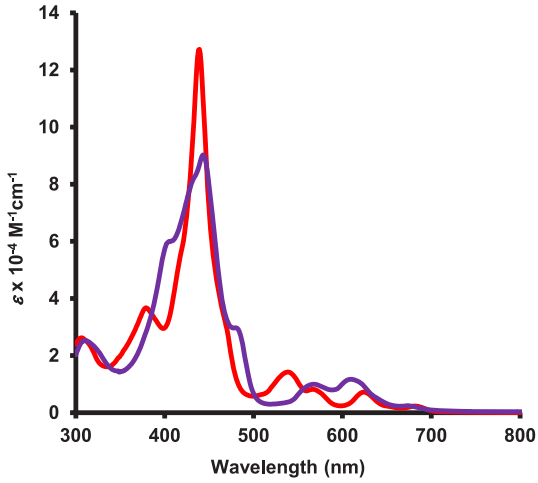


**Figure 3.** UV–vis spectra of 23-methylcarbaporphyrin **16** in 1% triethylamine–dichloromethane (free base, red line) and 1% TFA–dichloromethane (monocation **16**H$^+$, purple line).

porphyrinoid, showing a strong Soret absorption at 439 nm and Q bands at 538, 567, 624, and 683 nm. Addition of trifluoroacetic acid (TFA) afforded a monoprotonated species **16**H$^+$ that showed a diminished Soret band at 444 nm (Figure 3). Crystals of **16** that were suitable for X-ray crystallographic analysis were obtained, and the results showed that the pyrrole ring bearing the internal methyl group was tilted by 24.34(3)° from the macrocyclic plane, defined by atoms C1, C2, C3, C4, C5, C6, C7, C8, C9, C10, C11, C14, C15, C16, C17, C18, C19, C20, and C21 (Figure 4). The remainder of the

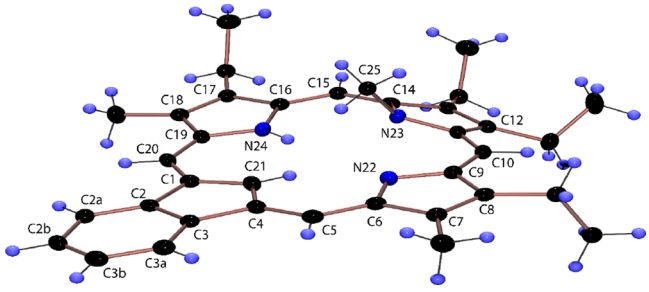


**Figure 4.** Color POV-Ray rendered ORTEP III drawing (50% probability level, hydrogen atoms rendered arbitrarily small for clarity) of 23-methylcarbaporphyrin **16**.

macrocyclic framework is rather flat, with the two remaining pyrrole rings and the indene subunit only tilted 0.46(3), 3.04(3), and 2.96(2)°, respectively, from the macrocyclic plane. In addition, the *N*-methyl bond is significantly bent relative to the pyrrole ring plane, as evidenced by the 139.2(1)° C12–C11–N23–C25 and 137.8(1)° C13–C14–N23–C25 torsion angles. These results differ from the structure obtained for a benzocarbaporphyrin without the *N*-alkyl substituent as this showed that the indene moiety was tilted by 15.5° relative to the mean macrocyclic plane, whereas


DOI: 10.1021/acs.organomet.8b00863
*Organometallics* XXXX, XXX, XXX–XXX

the pyrrole to mean macrocyclic plane tilts were 2.5, 4.4, and 4.9°.[35] With the exception of the C1−C2 bond length, a Mogul geometry check validated all bond distances, angles, and torsions to be within typical ranges.[36] The long 1.4822(19) Å C1−C2 and 1.4753(19) Å C3−C4 bond lengths are consistent with more single-bond-like character, which suggests the phenyl $\pi$-system of the indene subunit is isolated from the main macrocyclic $\pi$-system.

23-Methylcarbaporphyrin **16** was reacted with palladium(II) acetate in refluxing acetonitrile. When the reaction was carried out for 1 h, a mixture of metalated products was obtained. However, when the reaction was terminated after 5 min and the crude products were purified by column chromatography and recrystallized from chloroform−methanol, a *N*-methyl palladium complex **22** was isolated in 67% yield (Scheme 5).

**Scheme 5. Preparation of Palladium and Rhodium Organometallic Derivatives from 23-Methylcarbaporphyrin 16**

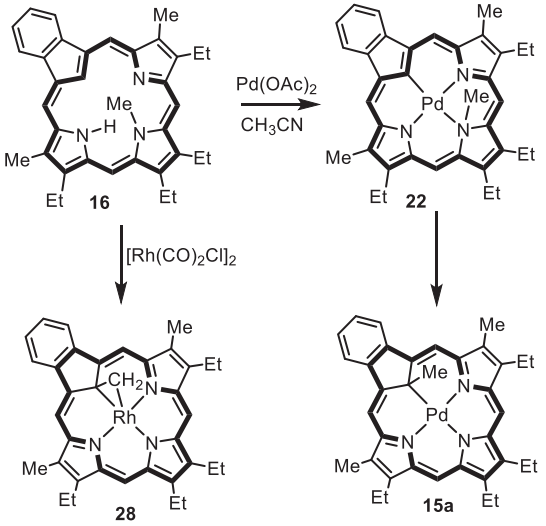


This species retained a strong aromatic ring current, showing the *meso*-protons downfield at 9.85 and 10.00 ppm and the internal methyl unit as an upfield singlet at −2.86 ppm. The symmetry of the complex was evident from both the proton and carbon-13 NMR spectra. The benzo unit gave rise to two 2H multiplets at 7.47 and 8.50 ppm, demonstrating that the complex has a similar conjugation pathway to **16**. The UV−vis spectrum of **22** was complex, giving several strong absorptions between 390 and 520 nm and additional broad peaks at higher wavelengths (Figure 5). When the reaction of **16** with palladium(II) acetate in refluxing acetonitrile was carried out for 16 h, the initially formed complex was completely converted to the C-methyl derivative **15a**. Hence, alkyl group migration still occurs for 23-methylcarbaporphyrin **16** but at a much slower rate. The 21-methyl complex was identical to the previously isolated product from the reaction of 22-methylcarbaporphyrin **12a** with $Pd(OAc)_2$.[21] The UV−vis spectrum for **15a** is quite different from **22**, showing a weakened Soret-like band at 421 nm and a fairly strong absorption at 697 nm (Figure 5). Although **15a** is aromatic, the conjugation pathway is redirected through the benzo unit. This causes the benzo-proton resonances to shift much further downfield to give multiplets at 8.24 and 9.41 ppm. The *meso*-protons for **15a** were identified as two 2H singlets at 9.56 and

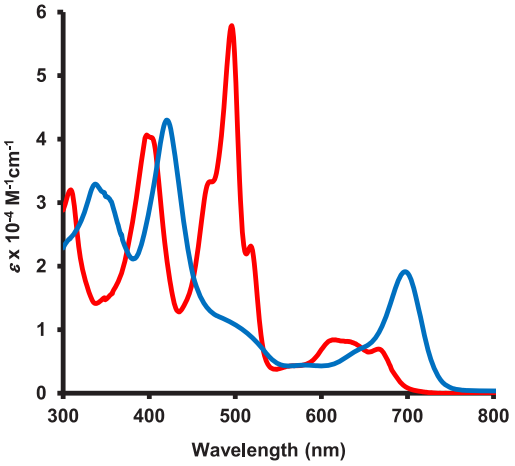


**Figure 5.** UV−vis spectra of palladium(II) carbaporphyrin complexes **22** (23-methyl, red line) and **15a** (21-methyl, blue line).

10.27 ppm, whereas the inner methyl group appeared upfield at −3.21 ppm. Again, the proton and carbon-13 NMR spectra were consistent with **15a** possessing a plane of symmetry. The structure of **15a** was confirmed by X-ray crystallography (Figure 6). The metrics of the framework bond distances are

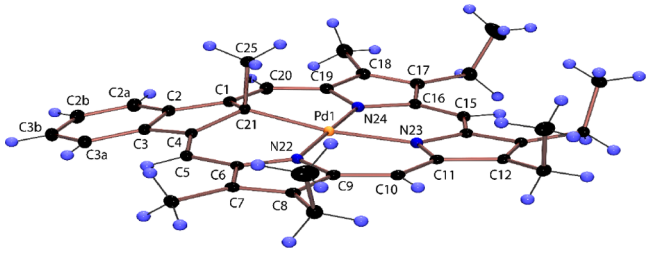


**Figure 6.** Color POV-Ray rendered ORTEP III drawing (50% probability level, hydrogen atoms rendered arbitrarily small for clarity) of palladium(II) 21-methylcarbaporphyrin **15a**.

consistent with an overall aromatic carbaporphyrin with a $sp^3$-hybridized C21. The palladium(II) center resides in an approximately square planar coordination environment with 2.058(2) Å Pd−C21, 2.037(2) Å Pd−N22, 2.066(2) Å Pd−N23, and 2.028(1) Å Pd−N24 bond lengths. In fact, the metal coordination environment is indistinguishable from that of the closely related complex (8,12,13,17-tetraethyl-2,3-bis(methoxycarbonyl)-7,18,21-trimethyl-21-carbaporphyrinato)palladium(II).[16] Complex **15a** has the palladium(II) ion coordinating $\eta^1$ to C21, and as the carbon is alkylated, this leads to the distended 1.491(2) and 1.498(2) Å $sp^3 \rightarrow sp^2$ C21−C1 and C21−C4 bond distances, and C21 is clearly separated from the macrocycle's $\pi$-system. This is supported by the nonplanar 7.8(2) and 8.9(2)° torsion angles observed, respectively, for C3−C2−C1−C21 and C2−C3−C4−C21, along with the C21 atom being located 0.360(2) Å out of the $PdN_3$ plane and 0.196(2) Å out of the plane defined by the other indene subunit atoms. The plane of the other indene subunit atoms is tilted 14.82(4)° from the $PdN_3$ plane. The C25 methyl group lies 1.935(2) Å out of the $PdN_3$ plane and 1.707(2) Å out of the plane defined by the other indene subunit atoms. The $sp^3$-hybridized C25 methyl group in **15a** is not available to interact with the palladium(II) metal center, as illustrated by the over 2.76 Å Pd···C(methyl) separation. The C25−C21−Pd bond angle is 98.1(1)°, and the C25−C21−C1


DOI: 10.1021/acs.organomet.8b00863
*Organometallics* XXXX, XXX, XXX−XXX

and C25−C21−C4 bond angles are 107.2(1) and 107.8(1)°, respectively. The C1−C2 and C3−C4 bond lengths for **15a** are ca. 0.03 Å shorter than those found in carbaporphyrin **16**, which is consistent with the aromatic delocalization pathway being relocated through the indene unit in the metalated derivative.

A time course experiment was conducted in order to gain further insights into the transformation of **22** into **15a**. The relative proportions of the two metallocarbaporphyrins were assessed by proton NMR spectroscopy by comparing the integrations for the *meso*-, benzo-, and internal methyl protons. Apart from **15a** and **22**, no other porphyrinoid species could be identified in the NMR spectra for these mixtures. The formation of **22** is evidently very rapid, but its conversion to **15a** was comparatively slow and was only 50% complete after refluxing for 2.5 h in acetonitrile (Figure S16). Although it is possible that **14a** could be an intermediate in the formation of **15a**, the presence of this species was not detected in any of the proton NMR spectra. As a slight excess of $Pd(OAc)_2$ is used to prepare these palladium complexes, there was a possibility that this promoted the rearrangement. However, the presence or absence of $Pd(OAc)_2$ had no measurable effect on the rate of conversion of **22** to **15a**. A second time course experiment was performed where **22** was dissolved in acetonitrile-$d_3$ at 70 °C (Figure 7). The data showed an inexorable conversion of **22** to

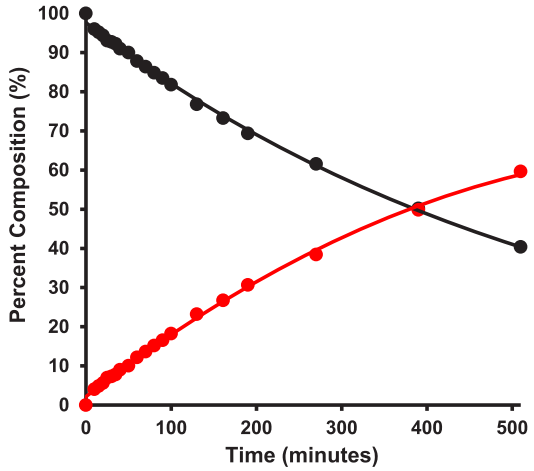


**Figure 7.** Time course experiment showing the conversion of **22** (black line) into the 21-methylcarbaporphyrin **15a** (red line). The experiment was carried out at 70 °C in acetonitrile-$d_3$ and was monitored by proton NMR spectroscopy.

**15a** that was 50% complete after ca. 380 min. The reaction still occurs, albeit much more slowly, at room temperature in solution or in the solid state. A crystalline sample of **22** that had been stored for approximately 1 year was completely converted into the 21-methyl derivative **15a**. The new results provide some insights into these rearrangements, but the mechanism remains ambiguous. It is possible that the 22-methyl palladium(II) complex is formed as an intermediate as the conversion of **14a** to **15a** is comparatively fast compared to the rearrangement of **22**. However, the intermediacy of a palladium−methyl complex is more plausible. We propose that an oxidative addition occurs to afford the palladium(IV) complex **23**, and a subsequent reductive transfer of the methyl unit to C21 then produces the observed product (Scheme 6).

**Scheme 6. Proposed Mechanism for Methyl Group Migration in Palladium(II) Carbaporphyrins**

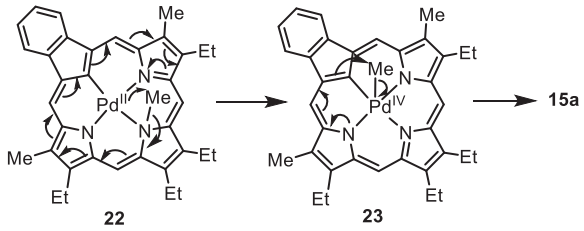


**Rhodium Complexes of Internally Alkylated Carbaporphyrins.** The synthesis, reactivity, and catalytic activity of rhodium porphyrins has been subjected to extensive investigations over the last 50 years.[37] Rhodium porphyrins have been used to selectively activate C−H and C−C bonds[38] and can catalyze enantioselective cyclopropanation reactions.[39] Rhodium(I) and rhodium(III) complexes of carbaporphyrins were only reported recently,[17] although examples of rhodium N-confused porphyrins[40] and azuliporphyrins[10] had been described earlier. Reaction of carbaporphyrin **2** with di-$\mu$-chlorotetracarbonyldirhodium(I) in refluxing dichloromethane afforded rhodium(I) complex **24** in up to 90% yield (Scheme 7).[17] When **24** was heated under reflux in pyridine,

**Scheme 7. Synthesis of Rhodium(I), Rhodium(III), and Iridium(III) Complexes of Carbaporphyrin 2**[17]

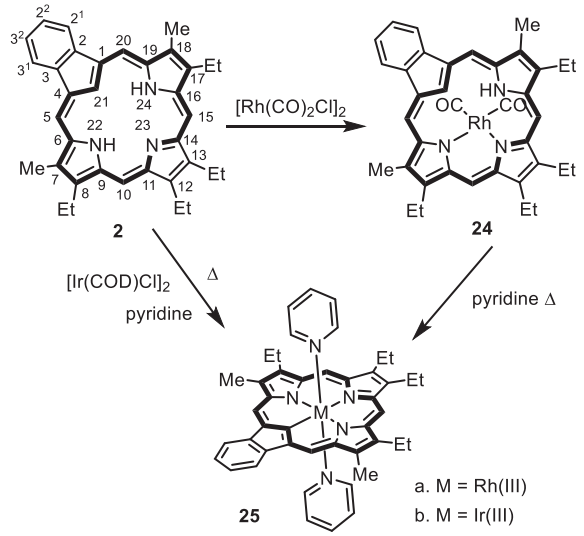


rhodium(III) complex **25a** was generated. A related iridium(III) derivative **25b** was also reported.[17] In order to investigate how the presence of internal alkyl substituents would influence this chemistry, 21-, 22-, and 23-methylcarbaporphyrins **13a**, **12a**, and **16** were reacted with $[Rh(CO)_2Cl]_2$ in refluxing dichloromethane. 22-Methylcarbaporphyrin **12a** reacted under these conditions to give rhodium(I) complex **26** in 50% yield (Figure 8). The complex retained fully aromatic properties, and the proton NMR spectrum for **26** showed the *meso*-protons downfield as four 1H singlets between 9.64 and 10.16 ppm (Figure 9). The external methyl substituents were significantly deshielded, producing two 3H singlets at 3.36 and 3.69 ppm, whereas the internal methyl and indene resonances appeared strongly upfield at −4.50 and −4.68 ppm, respectively. The carbon-13 NMR spectrum showed the carbonyl resonances as doublets at 178.8 and 179.4 ppm


DOI: 10.1021/acs.organomet.8b00863
*Organometallics* XXXX, XXX, XXX−XXX

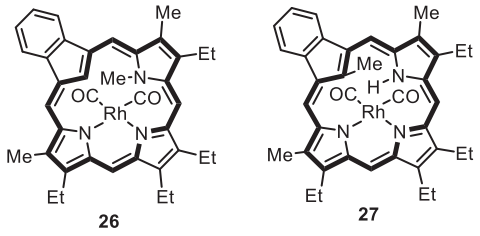


**Figure 8.** Rhodium(I) complexes of 22- and 21-methylcarbaporphyrins.

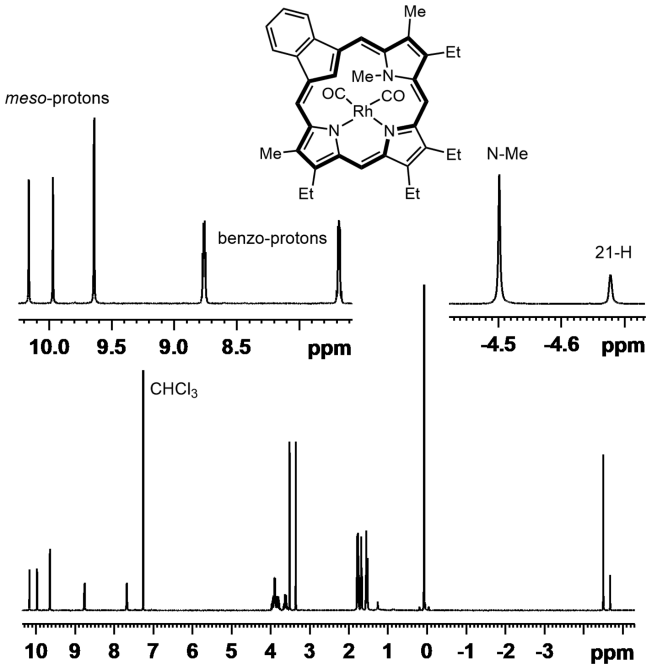


**Figure 9.** Proton NMR spectrum at 500 MHz of rhodium(I) 22-methylcarbaporphyrin complex **26**.

($^1J_{Rh-C}$ = ca. 69 Hz) due to coupling to rhodium-103 ($I = {}^1/_2$). The *meso*-carbons gave rise to four peaks at 97.1, 102.5, 104.6, and 106.6 ppm, and the internal indene CH appeared at 121.2 ppm. The presence of the carbonyl ligands was also evident from the IR spectrum due to the presence of two strong peaks at 1985 and 2057 $cm^{-1}$. The UV−vis spectrum for **26** afforded a Soret-like band at 481 nm and minor absorptions at 561 and 637 nm (Figure 10). 21-Methylcarbaporphyrin **13a** reacted similarly to give rhodium(I) complex **27** (Figure 8). The UV−vis spectrum of **27** afforded a similar UV−vis spectrum with a Soret-like band at 476 nm and weaker absorptions at 562, 627, and 604 nm. The proton NMR spectrum again confirmed that **27** is a highly diatropic species that no longer possesses a plane of symmetry. The *meso*-protons gave rise to four 1H singlets at 9.52, 9.56, 9.69, and 9.82 ppm, and the internal $CH_3$ and NH protons appeared upfield at −5.66 and −2.83 ppm, respectively. The benzo unit gave rise to multiplets between 7.3 and 8.2 ppm, indicating that the major aromatic $\pi$-delocalization pathway does not involve the arene moiety. The carbon-13 NMR spectrum again shows two doublets for the carbonyl ligands between 177 and 179 ppm, whereas the *meso*-carbons appeared at 93.0, 99.9, 103.5, and 108.6 ppm. In addition, the IR spectrum of **27** gave two peaks at 1996 and 2063 $cm^{-1}$ corresponding to the carbonyl units. Attempts to

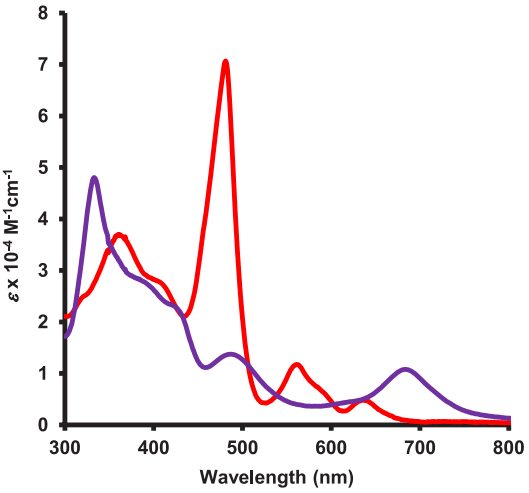


**Figure 10.** UV−vis spectra of rhodium(I) complex **26** (red line) and methylene-bridged rhodium(III) derivative **28** (purple line) in dichloromethane.

convert **26** or **27** into rhodium(III) complexes were unsuccessful.

The placement of the internal methyl substituent in **16** prevents the formation of rhodium(I) complexes of the type described above. Nevertheless, when **16** was reacted with $[Rh(CO)_2Cl]_2$ in refluxing toluene, a rhodium complex was generated in 31% yield (Scheme 5). The proton NMR spectrum for the new derivative showed a broad 2H doublet at −3.22 ppm ($^2J_{Rh-H}$ = 1 Hz) rather than an internal methyl substituent (Figure 11). The *meso*-protons were identified as

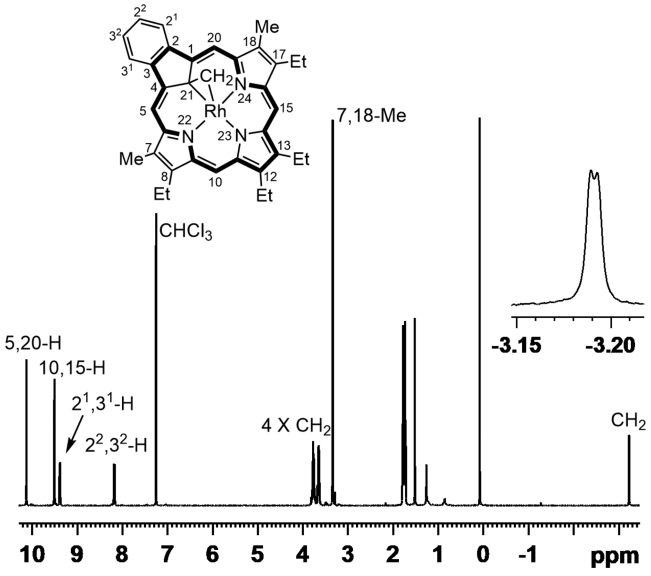


**Figure 11.** Proton NMR spectrum at 500 MHz of rhodium(III) complex **28**. The 2H resonance at −3.22 ppm due to the bridge $CH_2$ unit is coupled to $^{103}Rh$, and this gives rise to the observed doublet.

two 2H singlets at 9.51 and 10.13 ppm, confirming that the macrocycle retains strongly diatropic characteristics, and both the proton and carbon-13 NMR spectra show that the porphyrinoid has a plane of symmetry. Furthermore, the benzo-protons give rise to two 2H multiplets that are substantially shifted downfield to 8.18 and 9.39 ppm, which implies that the aromatic conjugation pathway passes through


DOI: 10.1021/acs.organomet.8b00863
Organometallics XXXX, XXX, XXX−XXX

this unit. These data are consistent with methylene-bridged rhodium(III) complex **28**. However, the electrospray ionization mass spectrum for this compound showed no sign of the proposed molecular ion and instead gave a base peak that corresponded to rhodium complex **29** (calcd for $C_{35}H_{34}N_3Rh$ *m*/*z* 599.1808; found 599.1805), together with additional peaks for unidentified species. The original analysis was carried out in the presence of 0.5% formic acid, but the same result was obtained when the formic acid was omitted. It is proposed that protonation and elimination of a methyl radical results in the formation of **29** (Scheme 8). Subsequent analysis of **28** by

**Scheme 8. Fragmentation of Rhodium Complex 28 during Analysis by ESI MS**

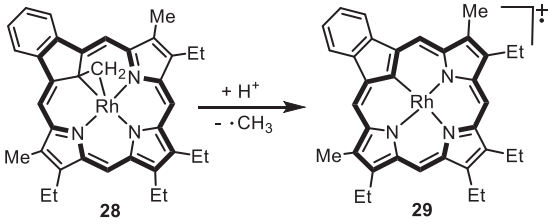


electron impact mass spectrometry gave a strong molecular ion at *m*/*z* 613 that matched the molecular formula for the methylene-bridged rhodium(III) complex. The formation of **28** from 23-methylcarbaporphyrin **16** was unexpected but presumably involves a rearrangement similar to the one observed for palladium(II) complex **22** where the *N*-methyl group effectively somersaults over the rhodium center. Related bridged rhodium(III) complexes were previously obtained by the ring contraction of benziporphyrin complexes.[41,42] The carbon-13 NMR spectrum of the rhodium(III) complex gave a doublet for the bridging $CH_2$ unit at 46.3 ppm ($^1J_{Rh-C}$ = 21.4 Hz), whereas the quaternary carbon at position 21 showed up as a doublet at 54.5 ppm ($^1J_{Rh-C}$ = 14.2 Hz). The *meso*-carbons afforded two resonances at 103.7 and 104.2 ppm. The UV−vis spectrum of **28** (Figure 10) was very different from rhodium(I) complexes **26** or **27**, showing a peak at 333 nm, followed by a series of broad absorptions culminating in a band that was centered on 682 nm. Although 18 $\pi$-electron delocalization pathways have been emphasized for palladium complexes **15** and the rhodium(III) derivative **28**, 22 $\pi$-electron circuits can also potentially contribute to these structures (see structures **15′** and **28′** in Figure 12). Indeed, these pathways help to explain the pronounced downfield shifts observed for the benzo-protons in the proton NMR spectra for these metalated derivatives, as well as the observed bathochromic shifts in the UV−vis spectra resulting from the macrocycle's extended chromophore.

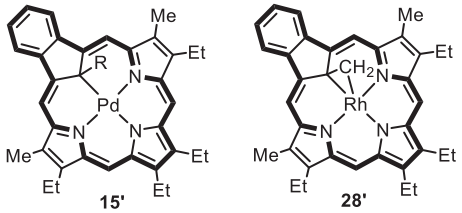


**Figure 12.** Alternative 22$\pi$-electron delocalization pathways for metallocarbaporphyrinoids **15** and **28**.

The structure of **28** was confirmed by X-ray crystallography (Figure 13). The porphyrinoid framework conformation is

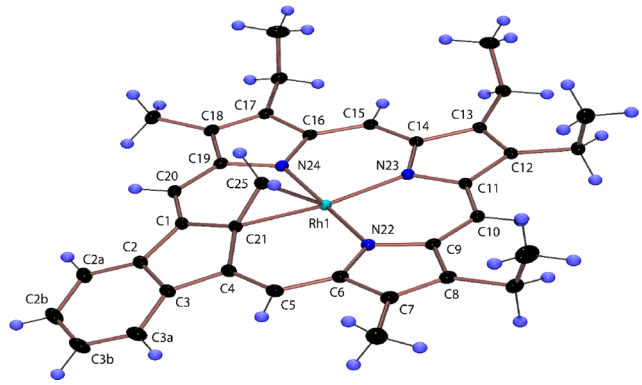


**Figure 13.** Color POV-Ray rendered ORTEP III drawing (50% probability level, hydrogen atoms rendered arbitrarily small for clarity) of methylene-bridged rhodium(III) carbaporphyrin **28**.

remarkably similar to that of palladium complex **15a**, the most obvious difference being the presence of the three-membered rhodacycle. The metrics of the framework bond distances are consistent with an overall aromatic carbaporphyrin with a $sp^3$-hybridized C21, and the C1−C2 and C3−C4 bond lengths of ca. 1.447 Å are consistent with the delocalization pathway passing through the indene unit. The C1−C21−C4 bond angle is 107.3(1)°, and the C25−C21−C1 and C25−C21−C4 bond angles are both 120.5(1)°. The C1−C21−Rh and C4−C21−Rh bond angles are both 119.8(1)°, and the C25−C21−Rh bond angle is 64.09(6)°. The rhodium(III) center resides in a strongly distorted square pyramidal coordination environment with the equatorial plane consisting of C21 and the three pyrrole nitrogen atoms, with 2.1329(11) Å Rh−C21, 2.0369(9) Å Rh−N22, 2.0431(9) Å Rh−N23, and 2.0410(9) Å Rh−N24 bond lengths. The metal coordination environment is very similar to that of a closely related tetraphenyl rhodium(III) carbaporphyrin complex,[41] although there are some notable differences. Like this complex, **28** has the rhodium(III) ion coordinating $\eta^2$ to C21 and C25. Attachment of the methylene group to C21 leads to the distended 1.463(2) and 1.462(2) Å $sp^3 \rightarrow sp^2$ C21−C1 and C21−C4 bond distances, which separates C21 from the macrocycle's $\pi$-system. This is supported by the nonplanar 3.1(1) and 3.8(1)° torsion angles observed, respectively, for C3−C2−C1−C21 and C2−C3−C4−C21, along with the C21 atom being located 0.412(1) Å out of the $RhN_3$ plane and 0.035(1) Å out of the plane defined by the other indene subunit atoms. The plane of the other indene subunit atoms is tilted 18.21(3)° from the $RhN_3$ plane. Methylene unit C25 lies 1.585(1) Å out of the $RhN_3$ plane and 0.872(1) Å out of the plane defined by the other indene subunit atoms. The $sp^3$-hybridized C25 methylene group in **28** is clearly interacting with the rhodium(III) metal center, as illustrated by the 1.9932(11) Å Rh···C25(methylene) separation. This is on the shorter end of the 2.09(4) Å distribution of 297 known Rh−$CH_2$ bond distances found in the Cambridge Structural Database (v5.39, Aug 2018 updates) and notably 0.04 Å shorter than the rhodium(III) tetraphenylcarbaporphyrin complex.[41]



DOI: 10.1021/acs.organomet.8b00863
*Organometallics* XXXX, XXX, XXX−XXX

## CONCLUSIONS

Metalation of a 23-methylcarbaporphyrin with palladium(II) acetate in refluxing acetonitrile has been shown to initially give the corresponding *N*-methyl palladium(II) complex, but this species gradually rearranges to generate a C-methyl palladium-(II) derivative. The *N*-methyl complex rearranges in the absence of palladium(II) acetate, and the process slowly proceeds at room temperature even in the solid state. A mechanism for this transformation is proposed that involves a transient palladium(IV) species. The 21- and 22-Methylcarbaporphyrins reacted with $[Rh(CO)_2Cl]_2$ to give rhodium(I) complexes, but the 23-methylcarbaporphyrin afforded a methylene-bridged rhodium(III) complex that had undergone a similar transformation to the one observed for the palladium series. These observations demonstrate that carbaporphyrin ligands facilitate unexpected reactivity that can lead to diverse organometallic structures.

## EXPERIMENTAL SECTION

Melting points are uncorrected. NMR spectra were recorded using a 400 or 500 MHz NMR spectrometer and were run at 302 K unless otherwise indicated. $^1$H NMR values are reported as chemical shifts $\delta$, relative integral, multiplicity (s, singlet; d, doublet; t, triplet; q, quartet; m, multiplet; br, broad peak), and coupling constant ($J$). Chemical shifts are reported in parts per million (ppm) relative to $CDCl_3$ ($^1$H residual $CHCl_3$ singlet $\delta$ 7.26, $^{13}$C $CDCl_3$ triplet $\delta$ 77.23) or DMSO-$d_6$ ($^1$H residual DMSO-$d_5$ pentet $\delta$ 2.49, $^{13}$C DMSO-$d_6$ septet $\delta$ 39.7), and coupling constants were taken directly from the spectra. NMR assignments were made with the aid of $^1$H−$^1$H COSY, HSQC, DEPT-135, and NOE difference proton NMR spectroscopy. The 2D experiments were performed using standard software. High-resolution mass spectra (HR-MS) were carried out using a double focusing magnetic sector instrument. $^1$H and $^{13}$C NMR spectra for all new compounds are reported in Supporting Information.

**Ethyl 3,4-Diethyl-1-methylpyrrole-2-carboxylate (17b).** 3-Acetoxy-4-nitrohexane (52.5 g, 0.278 mol) and ethyl isocyanoacetate (26.0 g, 0.230 mol) were mixed with THF (165 mL) and 2-propanol (67 mL) in a three-neck round-bottom flask fitted with a thermometer, addition funnel, and drying tube. DBU (86.0 g, 0.565 mol) was added dropwise, maintaining the temperature between 20 and 30 °C with the aid of a salt-ice bath. After the addition was complete, the orange solution was stirred at room temperature overnight. The solvent was removed under reduced pressure and the residue poured into water (225 mL). Diethyl ether (225 mL) was added and the aqueous layer drawn off and extracted twice with 225 mL of diethyl ether. The combined ether layers were washed with 10% aqueous HCl (2 × 300 mL), dried over magnesium sulfate, and the solvent removed on a rotary evaporator. The residue was vacuum distilled to yield ethyl 3,4-diethylpyrrole-2-carboxylate (**17a**)[43] (31.6 g, 0.162 mol, 70%) as a pale yellow oil: bp 102−105 °C at 0.6 Torr; $^1$H NMR (400 MHz, $CDCl_3$) $\delta$ 1.16 (3H, t, $^3J_{HH}$ = 7.5 Hz), 1.20 (3H, t, $^3J_{HH}$ = 7.5 Hz) (3,4-$CH_2CH_3$), 1.36 (3H, t, $^3J_{HH}$ = 7.2 Hz, $OCH_2CH_3$), 2.46 (2H, q, $^3J_{HH}$ = 7.5 Hz, 4−$CH_2CH_3$), 2.77 (2H, q, $^3J_{HH}$ = 7.5 Hz, 3−$CH_2CH_3$), 4.33 (2H, q, $^3J_{HH}$ = 7.2 Hz, $OCH_2$), 6.68 (1H, d, $^3J_{HH}$ = 2.9 Hz, 5-H), 9.00 (1H, br s, NH). The proton NMR spectrum shows the presence of ca. 3% of the corresponding isopropyl ester due to transesterification with 2-propanol.

Potassium hydroxide pellets (3.84 g) were heated with dimethylsulfoxide (15 mL) until a yellow solution was obtained. The solution was cooled to room temperature, and the foregoing pyrrole ester **17a** (3.80 g, 19.5 mmol) was added. After the mixture had been stirred for 1 h, methyl iodide (5.2 g) was added dropwise, keeping the temperature below 30 °C with the aid of a salt-ice bath. After the addition was completed, the solution was stirred for an additional 1 h, keeping the temperature below 30 °C. The solution was poured in ice/water (200 mL), and the aqueous layer was extracted with dichloromethane (2 × 200 mL). The combined dichloromethane layers were washed with water (5 × 100 mL), dried over magnesium sulfate, and the solvent removed under reduced pressure. The residue was vacuum distilled to yield *N*-methylpyrrole ester **17b** (3.20 g, 15.3 mmol, 79%) as a pale yellow oil: bp 98−100 °C at 1 Torr; $^1$H NMR (500 MHz, $CDCl_3$) $\delta$ 1.12 (3H, t, $^3J_{HH}$ = 7.6 Hz, 3-$CH_2CH_3$), 1.14 (3H, t, $^3J_{HH}$ = 7.6 Hz, 4-$CH_2CH_3$), 1.30 (3H, t, $^3J_{HH}$ = 7.2 Hz, $OCH_2CH_3$), 2.37 (2H, q, $^3J_{HH}$ = 7.6 Hz, 4−$CH_2CH_3$), 2.72 (2H, q, $^3J_{HH}$ = 7.6 Hz, 3−$CH_2CH_3$), 3.75 (3H, s, N-Me), 4.24 (2H, q, $^3J_{HH}$ = 7.2 Hz, $OCH_2$), 6.43 (1H, s, 5-H); $^{13}$C NMR (125 MHz, $CDCl_3$) $\delta$ 13.8 ($OCH_2CH_3$), 14.5 (4-$CH_2CH_3$), 15.2 (3-$CH_2CH_3$), 17.4 (4-$CH_2$), 18.5 (3-$CH_2$), 36.5 (N-Me), 58.7 ($OCH_2$), 118.6, 123.5, 125.8 (5-CH), 133.4, 161.2 (C═O); HR-MS (EI) $m/z$ calcd for $C_{12}H_{19}NO_2$ 209.1416; found 209.1419.

**3,4-Diethyl-1-methylpyrrole (18).** Pyrrole ester **17b** (2.82 g, 13.5 mmol) was added to sodium hydroxide (1.07 g) in ethylene glycol (11 mL), and the mixture was heated for 2.5 h at 200 °C. After being cooled to room temperature, the mixture was partitioned between water (50 mL) and hexanes (50 mL). The aqueous layer was drawn off and further extracted with hexanes (3 × 50 mL). The combined hexanes layers were dried over magnesium sulfate, and the solvent was removed under reduced pressure to yield 3,4-diethyl-1-methylpyrrole (1.55 g, 11.3 mmol, 84%) as a pale yellow oil: bp 78−80 °C at 18 Torr; $^1$H NMR (500 MHz, $CDCl_3$) $\delta$ 1.46 (6H, t, $^3J_{HH}$ = 7.6 Hz, 2 × $CH_2CH_3$), 2.71 (4H, q, $^3J_{HH}$ = 7.6 Hz, 2 × $CH_2CH_3$), 3.80 (3H, s, N-Me), 6.58 (2H, s, 2,5-H); $^{13}$C NMR (125 MHz, $CDCl_3$) $\delta$ 14.6 (2 × $CH_2CH_3$), 18.3 (2 × $CH_2CH_3$), 35.1 (N-Me), 118.2 (2,5-CH), 124.1 (3,4-C); HR-MS (EI) $m/z$ calcd for $C_9H_{15}N$ 137.1204; found 137.1204.

**2,5-Bis(5-benzyloxycarbonyl-3-ethyl-4-methyl-2-pyrrolylmethyl)-3,4-diethyl-1-methylpyrrole (20a).** Benzyl 5-acetoxymethyl-4-ethyl-3-methylpyrrole-2-carboxylate (1.28 g, 4.10 mmol) and 3,4-diethyl-1-methylpyrrole (0.279 g, 2.04 mmol) were dissolved in acetonitrile (15 mL) and acetic acid (1 mL). The mixture was refluxed overnight under nitrogen. The solution was then cooled to room temperature, diluted with dichloromethane (50 mL), and then washed with water (100 mL) and aqueous 10% sodium bicarbonate solution (100 mL). The dichloromethane layer was dried over sodium sulfate and the solvent removed under reduced pressure. The residue was purified by column chromatography on silica gel, eluting with 80:20:1 dichloromethane/hexanes/triethylamine, and afforded the *N*-methyl tripyrrane (0.624 g, 0.964 mmol, 48%) as an orange oil that slowly solidified when stored in the freezer: $^1$H NMR (500 MHz, $CDCl_3$) $\delta$ 1.05 (6H, t, $^3J_{HH}$ = 7.6 Hz, 3′,3″-$CH_2CH_3$), 1.09 (6H, t, $^3J_{HH}$ = 7.6 Hz, 3,4-$CH_2CH_3$), 2.27 (6H, s, 4′,4″-$CH_3$), 2.39−2.45 (8H, m, 4 × $CH_2CH_3$), 2.98 (3H, s, N-Me), 3.81 (4H, s, 2 × bridge-$CH_2$), 5.24 (4H, s, 2 × $OCH_2$), 7.28−7.39 (10H, m, 2 × Ph), 8.23 (2H, br s, 2 × NH); $^{13}$C NMR (125 MHz, $CDCl_3$) $\delta$ 10.7 (4′,4″-Me), 15.4 (3′,3″-$CH_2CH_3$), 17.24 (3,4-$CH_2CH_3$), 17.28, 18.0 (4 × $CH_2CH_3$), 21.9 (2 × bridge-$CH_2$), 30.4 (N-Me), 65.6 (2 × $OCH_2$), 117.1, 122.2, 122.9, 123.4, 128.1 (Ph), 128.7 (Ph), 131.1, 136.9, 161.6 (2 × C═O). HR-MS (ESI) $m/z$ [M + H]$^+$ calcd for $C_{41}H_{50}N_3O_4$ 648.3801; found 648.3792.

***N*-Methyl Tripyrrane Dicarboxylic Acid 20b.** *N*-Methyl tripyrrane **20a** (0.703 g, 1.09 mmol) was placed in a hydrogenation vessel and dissolved in acetone (100 mL), methanol (34 mL), and triethylamine (14 drops). The mixture was purged with nitrogen; 10% palladium charcoal (67 mg) was added and the solution shaken under an atmosphere of 40 psi hydrogen at room temperature overnight. The catalyst was removed by suction filtration and the solvent removed on a rotary evaporatory while maintaining the bath temperature below 30 °C. The residue was dissolved in 5% aqueous ammonium and diluted to a final volume of 50 mL with water. The resulting solution was cooled to 0−5 °C and then acidified by adding acetic acid dropwise while maintaining the temperature below 5 °C. The mixture was allowed to sit in a salt-ice bath for 30 min, and the precipitate was then collected by suction filtration and washed multiple times with water to remove all traces of acid. The solid was dried overnight in a vacuum desiccator to yield the dicarboxylic acid (0.419 g, 0.897 mmol, 83%) as an unstable pale purple powder that was used without further purification; $^1$H NMR (500 MHz, DMSO-


DOI: 10.1021/acs.organomet.8b00863
Organometallics XXXX, XXX, XXX−XXX

$d_6$) $\delta$ 0.73 (6H, t, $^3J_{HH}$ = 7.5 Hz), 0.97 (6H, t, $^3J_{HH}$ = 7.5 Hz) (4 × $CH_2CH_3$), 2.12 (6H, s, 4′,4″-$CH_3$), 2.11 (4H, q, $^3J_{HH}$ = 7.5 Hz), 2.35 (4H, q, $^3J_{HH}$ = 7.5 Hz) (4 × $CH_2CH_3$), 2.99 (3H, s, N-Me), 3.81 (4H, s, 2 × bridge-$CH_2$), 10.14 (2H, br s, 2 × NH), 11.53 (2H, v br, 2 × $CO_2H$); $^{13}$C NMR (125 MHz, $CDCl_3$) $\delta$ 9.9 (4′,4′′-Me), 14.8, 16.3, 16.5, 17.2, 21.6 (2 × bridge-$CH_2$), 30.1 (N-Me), 116.5, 119.6, 122.6, 123.1, 125.5, 130.4, 162.1 (2 × C═O); HR-MS (ESI) $m/z$ calcd for $C_{27}H_{37}N_3O_4$ 490.2682; found 490.2672.

**8,12,13,17-Tetraethyl-7,18,23-trimethylbenzo[*b*]-carbaporphyrin (16).** *N*-Methyl tripyrrane dicarboxylic acid **20b** (0.144 g, 0.308 mmol) was dissolved in TFA (1.5 mL) and stirred under nitrogen for 2 min. Dichloromethane (27 mL) was added, followed immediately by indene dialdehyde (54.0 mg, 0.314 mmol), and the solution was stirred under nitrogen for 2 h. The mixture was neutralized by the dropwise addition of triethylamine; DDQ (72.0 mg, 0.317 mmol) was added, and the mixture was stirred for a further 1 h. The solution was washed with water (100 mL) and then sodium bicarbonate (100 mL), and the solvent was removed under reduced pressure. The residue was chromatographed twice on grade 3 neutral alumina eluting with dichloromethane and then chloroform, and a dark brown band was collected. The product was recrystallized from chloroform−methanol to yield the 23-methylbenzocarbaporphyrin (52.5 mg, 0.102 mmol, 32%) as dark purple-blue crystals: mp >300 °C; UV−vis (1% $Et_3N$−$CH_2Cl_2$) $\lambda_{max}$/nm (log $\varepsilon$) 306 (4.42), 379 (4.56), 439 (5.10), 538 (4.15), 567 (3.91), 624 (3.86), 683 (3.36); UV−vis (1% TFA−$CH_2Cl_2$) $\lambda_{max}$/nm (log $\varepsilon$) 310 (4.42), 403 (sh, 4.77), 444 (4.97), 481 (4.47), 568 (4.01), 608 (4.08), 677 (3.26); $^1$H NMR (500 MHz, $CDCl_3$) $\delta$ −4.95 (1H, s, 21-H), −4.25 (3H, s, N-Me), −0.63 (1H, v br, NH), 1.47 (6H, t, $^3J_{HH}$ = 7.7 Hz, 12,13-$CH_2CH_3$), 1.83 (6H, t, $^3J_{HH}$ = 7.7 Hz, 8,17-$CH_2CH_3$), 3.51 (6H, s, 7,18-Me), 3.67−3.75 (2H, m), 3.76−3.84 (2H, m) (12,13-$CH_2$), 3.88−4.02 (4H, m, 8,17-$CH_2$), 7.67−7.71 (2H, m, $2^2$,$3^2$-H), 8.79−8.83 (2H, m, $2^1$,$3^1$-H), 9.67 (2H, s, 10,15-H), 10.03 (2H, s, 5,20-H); $^1$H NMR (500 MHz, TFA-$CDCl_3$) $\delta$ −6.53 (1H, br s, 21-H), −4.79 (2H, s, 2 × NH), −4.51 (3H, s, N-Me), 1.50 (6H, t, $^3J_{HH}$ = 7.7 Hz, 12,13-$CH_2CH_3$), 1.77 (6H, t, $^3J_{HH}$ = 7.7 Hz, 8,17-$CH_2CH_3$), 3.60 (6H, s, 7,18-Me), 3.69−3.80 (4H, m, 12,13-$CH_2$), 4.05 (4H, q, $^3J_{HH}$ = 7.7 Hz, 8,17-$CH_2$), 7.70−7.80 (2H, br, $2^2$,$3^2$-H), 8.64−8.72 (2H, m, $2^1$,$3^1$-H), 10.00 (2H, s, 10,15-H), 10.26 (2H, s, 5,20-H); $^{13}$C NMR (125 MHz, $CDCl_3$) $\delta$ 11.5 (7,18-Me), 16.9 (12,13-$CH_2CH_3$), 17.4 (8,17-$CH_2CH_3$), 20.0 (8,17-$CH_2$), 20.1 (12,13-$CH_2$), 31.4 (N-Me), 96.4 (10,15-CH), 103.4 (5,20-CH), 118.8 (21-CH), 120.4 ($2^1$,$3^1$-CH), 126.5 ($2^2$,$3^2$-CH), 134.2, 135.2, 136.3, 140.7, 144.0, 147.6; $^{13}$C NMR (125 MHz, TFA-$CDCl_3$) $\delta$ 11.7 (7,18-Me), 16.5 (12,13-$CH_2CH_3$), 16.9 (8,17-$CH_2CH_3$), 20.13, 20.15 (4 × $CH_2CH_3$), 30.7 (N-Me), 95.8 (10,15-CH), 103.6 (5,20-CH), 116.5 (21-CH), 121.9 ($2^1$,$3^1$-CH), 128.7 ($2^2$,$3^2$-CH), 136.2, 136.8, 138.8, 138.9, 140.6, 141.5, 141.7, 150.6; HR-MS (ESI) $m/z$ $[M + H]^+$ calcd for $C_{36}H_{40}N_3$ 514.3222; found 514.3198.

**[8,12,13,17-Tetraethyl-7,18,23-trimethylbenzo[*b*]-carbaporphyrinato]palladium(II) (22).** Palladium(II) acetate (10.0 mg, 0.0450 mmol) was added to a solution of 23-methylbenzocarbaporphyrin **16** (10.0 mg, 0.0195 mmol) in acetonitrile (10 mL) and heated under reflux in a preheated oil bath for 5 min. The solution was diluted with chloroform (30 mL) and washed with water (50 mL). The aqueous solution was back extracted with chloroform, and the combined organic layers were evaporated under reduced pressure. The residue was purified by column chromatography on silica gel eluting with dichloromethane/hexanes (70:30), and a dark green band was collected. The solvent was removed on a rotary evaporator and the residue recrystallized from chloroform−methanol to give the palladium complex (8.0 mg, 0.013 mmol, 67%) as dark green crystals: mp >300 °C; UV−vis ($CH_2Cl_2$) $\lambda_{max}$/nm (log $\varepsilon$) 309 (4.50), 397 (4.61), 404 (sh, 4.60), 470 (sh, 4.52), 496 (4.76), 518 (4.36), 561 (3.63), 613 (3.93), 635 (sh, 3.90), 667 (3.84); $^1$H NMR (500 MHz, $CDCl_3$) $\delta$ −2.86 (3H, s, N-Me), 1.67 (6H, t, $^3J_{HH}$ = 7.7 Hz, 12,13-$CH_2CH_3$), 1.81 (6H, t, $^3J_{HH}$ = 7.7 Hz, 8,17-$CH_2CH_3$), 3.48 (6H, s, 7,18-Me), 3.84−4.00 (8H, m, 4 × $CH_2CH_3$), 7.45−7.49 (2H, m, $2^2$,$3^2$-H), 8.48−8.52 (2H, m, $2^1$,$3^1$-H), 9.85 (2H, s, 10,15-H), 10.00 (2H, s, 5,20-H); $^{13}$C NMR (125 MHz, $CDCl_3$) $\delta$ 11.7 (7,18-Me), 16.5 (12,13-$CH_2CH_3$), 17.6 (8,17-$CH_2CH_3$), 20.16, 20.21 (4 × $CH_2CH_3$), 45.3 (N-Me), 98.9 (10,15-CH), 109.6 (5,20-CH), 118.8 ($2^1$,$3^1$-CH), 126.0 ($2^2$,$3^2$-CH), 133.8, 135.1, 136.3, 138.9, 140.7, 142.7, 145.6, 149.8; HR-MS (ESI) $m/z$ calcd for $C_{36}H_{37}N_3Pd$ 617.2022; found 617.2044.

**[8,12,13,17-Tetraethyl-7,18,21-trimethylbenzo[*b*]-carbaporphyrinato]palladium(II) (15a).** Palladium(II) acetate (10 mg, 0.0450 mmol) was added to a solution of 23-methylbenzocarbaporphyrin **16** (10 mg, 0.0195 mmol) in acetonitrile (10 mL) and the mixture refluxed overnight. The solvent was removed under reduced pressure and the residue chromatographed on a silica gel column eluting with dichloromethane/hexanes (70:30). A brown band was collected and the solvent removed under reduced pressure to give **15a** (10.2 mg, 0.0165 mmol, 85%) as a dark brown solid: mp >300 °C; $^1$H NMR (500 MHz, $CDCl_3$) $\delta$ −3.21 (3H, s, 21-$CH_3$), 1.74 (6H, t, $^3J_{HH}$ = 7.7 Hz), 1.75 (6H, t, $^3J_{HH}$ = 7.7 Hz) (4 × $CH_2CH_3$), 3.33 (6H, s), 3.71−3.78 (8H, m, 4 × $CH_2CH_3$), 8.22−8.25 (2H, m, $2^2$,$3^2$-H), 9.39−9.43 (2H, m, $2^1$,$3^1$-H), 9.56 (2H, s, 10,15-H), 10.27 (2H, s, 5,20-H). The sample had identical spectroscopic properties to a previously prepared sample obtained by reacting **12a** with Pd-$(OAc)_2$.[21]

**[8,12,13,17-Tetraethyl-7,18,22-trimethylbenzo[*b*]-carbaporphyrinato](dicarbonyl)rhodium(I) (26).** 22-Methylbenzocarbaporphyrin **12a** (10.4 mg, 0.0203 mmol) was dissolved in dichloromethane (22 mL) under nitrogen. Anhydrous sodium acetate (16.3 mg) was added, followed by $[Rh(CO)_2Cl]_2$ (7.8 mg, 0.0201 mmol), and the mixture was refluxed overnight under nitrogen. The solvent was removed under reduced pressure, and the residue was purified by column chromatography on silica gel eluting with dichloromethane/hexanes (50:50). The rhodium complex was collected as a brown band. Recrystallization from chloroform/hexanes afforded **26** (6.8 mg, 0.010 mmol, 50%) as dark crystals: mp >300 °C; UV−vis ($CH_2Cl_2$) $\lambda_{max}$/nm (log $\varepsilon$) 319 (sh, 4.39), 360 (4.57), 407 (sh, 4.44), 481 (4.85), 561 (4.07), 586 (sh, 3.83), 637 (3.68); IR (ZnSe) $\nu_{CO}$ 1985, 2057 cm$^{-1}$; $^1$H NMR (500 MHz, $CDCl_3$) $\delta$ −4.68 (1H, s, 21-H), −4.50 (3H, s, N-Me), 1.56 (3H, t, $^3J_{HH}$ = 7.7 Hz), 1.68 (3H, t, $^3J_{HH}$ = 7.7 Hz), 1.76 (3H, t, $^3J_{HH}$ = 7.7 Hz), 1.79 (3H, t, $^3J_{HH}$ = 7.7 Hz) (4 × $CH_2CH_3$), 3.36 (3H, s), 3.52 (3H, s) (7,18-Me), 3.56−3.69 (2H, m), 3.76−3.99 (6H, m) (4 × $CH_2CH_3$), 7.66−7.71 (2H, m, $2^2$,$3^2$-H), 8.74−8.78 (2H, m, $2^1$,$3^1$-H), 9.640 (1H, s), 9.643 (1H, s) (10,15-H), 9.97 (1H, s), 10.16 (1H, s) (5,20-H); $^{13}$C NMR (125 MHz, $CDCl_3$) $\delta$ 12.0, 12.3, 15.8, 17.6, 18.3, 18.4, 19.9, 20.0, 20.1, 20.6, 97.1, 102.5, 104.6, 106.6, 120.32, 120.35, 121.2 (br), 126.6, 130.1, 132.3, 132.9, 134.8, 136.5, 139.2, 139.4, 142.2, 143.7, 144.4, 147.8, 148.4, 149.1, 150.0, 152.5, 155.0, 178.8 (d, $^1J_{RhC}$ = 68.5 Hz, CO), 179.4 (d, $^1J_{RhC}$ = 69.4 Hz, CO); HR-MS (ESI) $m/z$ $[M + H]^+$ calcd for $C_{38}H_{39}N_3O_2Rh$ 672.2097; found 672.2104.

**[8,12,13,17-Tetraethyl-7,18,21-trimethylbenzo[*b*]-carbaporphyrinato](dicarbonyl)rhodium(I) (27).** Anhydrous sodium acetate (11.4 mg) was added, followed by $[Rh(CO)_2Cl]_2$ (5.5 mg, 0.0142 mmol), to a solution of 21-methylbenzocarbaporphyrin **13a** (7.0 mg, 0.0136 mmol) in dichloromethane (15 mL) under nitrogen. The resulting mixture was heated under reflux overnight. The solvent was removed under reduced pressure and the residue purified by column chromatography on silica gel eluting with dichloromethane/hexanes (50:50). The complex eluted as a green band. Recrystallization from chloroform/hexanes gave the rhodium(I) complex (6.2 mg, 0.00924 mmol, 67%) as as dark crystals: mp >300 °C; UV−vis ($CH_2Cl_2$) $\lambda_{max}$/nm (log $\varepsilon$) 327 (4.18), 368 (4.34), 476 (4.56), 562 (3.71), 604 (3.71), 627 (3.64); IR (ZnSe) $\nu_{CO}$ 1996, 2063 cm$^{-1}$; $^1$H NMR (500 MHz, $CDCl_3$) $\delta$ −5.66 (3H, s, N-Me), −2.83 (1H, br s, NH), 1.69 (3H, t, $^3J_{HH}$ = 7.7 Hz), 1.78−1.83 (9H, 3 overlapping triplets) (4 × $CH_2CH_3$), 3.35 (3H, s), 3.52 (3H, s) (7,18-Me), 3.67−3.85 (3H, m), 3.88−4.01 (5H, m) (4 × $CH_2CH_3$), 7.35 (1H, dt, $^4J_{HH}$ = 0.9 Hz, $^3J_{HH}$ = 7.3 Hz), 7.41 (1H, dt, $^4J_{HH}$ = 0.9 Hz, $^3J_{HH}$ = 7.4 Hz) ($2^2$,$3^2$-H), 7.97 (1H, d, $^3J_{HH}$ = 7.2 Hz), 8.20 (1H, d, $^3J_{HH}$ = 7.3 Hz) ($2^1$,$3^1$-H), 9.52 (1H, s), 9.56 (1H, s, 10,15-H), 9.69 (1H, s), 9.82 (1H, s) (5,20-H); $^{13}$C NMR (125 MHz, $CDCl_3$) $\delta$ 11.5, 11.8 (21-Me), 12.3, 17.4, 17.6, 18.0, 18.3, 19.75, 19.84, 19.91, 20.5, 93.0, 99.9, 103.5, 108.6, 120.0, 120.2, 126.1, 126.2, 127.8, 131.5,


DOI: 10.1021/acs.organomet.8b00863
*Organometallics* XXXX, XXX, XXX−XXX

132.8, 132.89, 132.94, 134.7, 136.1, 137.5, 139.1, 139.9, 140.1, 141.6, 143.2, 145.8, 147.7, 153.1, 154.8, 177.6 (d, $^1J_{RhC}$ = 67.0 Hz, CO), 179.0 (d, $^1J_{RhC}$ = 66.2 Hz, CO); HR-MS (ESI) $m/z$ $[M + H]^+$ calcd for $C_{38}H_{39}N_3O_2Rh$ 672.2097; found 672.2088.

**[8,12,13,17-Tetraethyl-7,18-dimethyl-21-methylenebenzo-[*b*]carbaporphyrinato]rhodium(III) (28).** 23-Methylbenzocarbaporphyrin **16** (20.0 mg, 0.0390 mmol) was dissolved in toluene (40 mL) under nitrogen. Anhydrous sodium acetate (33.3 mg) was added, followed by $[Rh(CO)_2Cl]_2$ (14.3 mg, 0.0368 mmol), and the mixture refluxed overnight. The solvent was removed under reduced pressure, and the residue was purified twice by column chromatography on silica gel eluting with dichloromethane. The product eluted as a dark band. Recrystallization from chloroform−methanol gave the rhodium(III) complex (7.4 mg, 0.0121 mmol, 31%) as dark crystals: mp >300 °C; UV−vis ($CH_2Cl_2$) $\lambda_{max}$/nm (log $\varepsilon$) 333 (4.68), 386 (sh, 4.45), 424 (sh, 4.36), 486 (4.14), 682 (4.03); $^1$H NMR (400 MHz, $CDCl_3$) $\delta$ −3.22 (2H, br d, $^2J_{RhH}$ = 1.0 Hz, Rh-$CH_2$), 1.74 (6H, t, $^3J_{HH}$ = 7.7 Hz, 8,17-$CH_2CH_3$), 1.78 (6H, t, $^3J_{HH}$ = 7.7 Hz, 12,13-$CH_2CH_3$), 3.34 (6H, s, 7,18-Me), 3.62−3.70 (4H, m, 8,17-$CH_2$), 3.72−3.83 (4H, m, 12,13-$CH_2$), 8.16−8.20 (2H, m, $2^2$,$3^2$-H), 9.37−9.41 (2H, m, $2^1$,$3^1$-H), 9.51 (2H, s, 10,15-H), 10.12 (2H, s, 5,20-H); $^{13}$C NMR (125 MHz, $CDCl_3$) $\delta$ 11.6 (7,18-Me), 17.4 (8,17-$CH_2CH_3$), 18.5 (12,13-$CH_2CH_3$), 19.6 (12,13-$CH_2$), 19.9 (8,17-$CH_2$), 46.3 (d, $^1J_{RhC}$ = 21.4 Hz, Rh-$CH_2$), 54.5 (d, $^1J_{RhC}$ = 14.2 Hz, 21-C), 103.7 (10,15-CH), 104.2 (5,20-CH), 121.3 ($2^1$,$3^1$-CH), 127.3 ($2^2$,$3^2$-CH), 135.8, 140.2, 141.7, 142.4, 144.3, 145.4, 149.6, 154.9; HR-MS (EI) $m/z$ calcd for $C_{36}H_{36}N_3Rh$ 613.1964; found 613.1659.

## ■ ASSOCIATED CONTENT

### Supporting Information

The Supporting Information is available free of charge on the ACS Publications website at DOI: 10.1021/acs.organomet.8b00863.

Experimental details for the X-ray crystallography and selected UV−vis, IR, $^1$H NMR, $^1$H−$^1$H COSY, HSQC, DEPT-135, $^{13}$C NMR, and mass spectra (PDF)

### Accession Codes

CCDC 1877450−1877452 contain the supplementary crystallographic data for this paper. These data can be obtained free of charge via www.ccdc.cam.ac.uk/data_request/cif, or by emailing data_request@ccdc.cam.ac.uk, or by contacting The Cambridge Crystallographic Data Centre, 12 Union Road, Cambridge CB2 1EZ, UK; fax: +44 1223 336033.

## ■ AUTHOR INFORMATION


### Corresponding Author

*E-mail: tdlash@ilstu.edu.

### ORCID

Timothy D. Lash: 0000-0002-0050-0385


### Notes

The authors declare no competing financial interest.

## ■ ACKNOWLEDGMENTS

This work was supported by the National Science Foundation under Grant No. CHE-1465049 and the Petroleum Research Fund, administered by the American Chemical Society. The authors also thank NSF-CHE (Grant No. 1039689) for funding the X-ray diffractometer.

## ■ REFERENCES


(1) Mironov, A. Transition Metal Complexes of Porphyrins and Porphyrinoids. In *Handbook of Porphyrin Science - With Applications to Chemistry, Physics, Material Science, Engineering, Biology and Medicine*; Kadish, K. M., Smith, K. M., Guilard, R., Eds.; World Scientific Publishing, 2012; Vol. *18*, pp 303−413.

(2) (a) Gupta, I.; Ravikanth, M. Recent Developments in Heteroporphyrins and their Analogues. *Coord. Chem. Rev.* **2006**, *250*, 468−518. (b) Chmielewski, P. J.; Latos- Grazyński, L. Core Modified Porphyrins − a Macrocyclic Platform for Organometallic Chemistry. *Coord. Chem. Rev.* **2005**, *249*, 2510−2533.

(3) (a) Lash, T. D. Carbaporphyrins and Related Systems. Synthesis, Characterization, Reactivity and Insights into the Nature of Porphyrinoid Aromaticity. In *Handbook of Porphyrin Science - With Applications to Chemistry, Physics, Material Science, Engineering, Biology and Medicine*; Kadish, K. M., Smith, K. M., Guilard, R., Eds.; World Scientific Publishing, 2012; Vol. *16*, pp 1−329. (b) Lash, T. D. Carbaporphyrinoid Systems. *Chem. Rev.* **2017**, *117*, 2313−2446.

(4) (a) Srinivasan, A.; Furuta, H. Confusion Approach to Porphyrinoid Chemistry. *Acc. Chem. Res.* **2005**, *38*, 10−20. (b) Toganoh, M.; Furuta, H. Blooming of Confused Porphyrinoids − Fusion, Expansion, Contraction, and More Confusion. *Chem. Commun.* **2012**, *48*, 937−954.

(5) Lash, T. D. Out of the Blue! Azuliporphyrins and Related Carbaporphyrinoid Systems. *Acc. Chem. Res.* **2016**, *49*, 471−482.

(6) Lash, T. D. Benziporphyrins, a Unique Platform for Exploring the Aromatic Characteristics of Porphyrinoid Systems. *Org. Biomol. Chem.* **2015**, *13*, 7846−7878.

(7) Lash, T. D. Metal Complexes of Carbaporphyrinoid Systems. *Chem. - Asian J.* **2014**, *9*, 682−705.

(8) (a) Graham, S. R.; Ferrence, G. M.; Lash, T. D. Organometallic Chemistry of Carbaporphyrinoids: Synthesis and Characterization of Nickel(II) and Palladium(II) Azuliporphyrins. *Chem. Commun.* **2002**, *38*, 894−895. (b) Lash, T. D.; Colby, D. A.; Graham, S. R.; Ferrence, G. M.; Szczepura, L. F. Organometallic Chemistry of Azuliporphyrins: Synthesis, Spectroscopy, Electrochemistry and Structural Characterization of Nickel(II), Palladium(II) and Platinum(II) Complexes of Azuliporphyrins. *Inorg. Chem.* **2003**, *42*, 7326−7338.

(9) Bialek, M. J.; Latos- Grazyński, L. Merging of Inner and Outer Ruthenium Organometallic Coordination Motifs within an Azuliporphyrin Framework. *Chem. Commun.* **2014**, *50*, 9270−9272.

(10) Stateman, L. M.; Ferrence, G. M.; Lash, T. D. Rhodium(III) Azuliporphyrins. *Organometallics* **2015**, *34*, 3842−3848.

(11) Lash, T. D.; Pokharel, K.; Zeller, M.; Ferrence, G. M. Iridium(III) Azuliporphyrins. *Chem. Commun.* **2012**, *48*, 11793−11795.

(12) Stepien, M.; Latos-Grazyński, L. Benziporphyrins: Exploring Arene Chemistry in a Macrocyclic Environment. *Acc. Chem. Res.* **2005**, *38*, 88−98.

(13) (a) Toganoh, M.; Furuta, H. In *Handbook of Porphyrin Science − With Applications to Chemistry, Physics, Material Science, Engineering, Biology and Medicine*; Kadish, K. M., Smith, K. M., Guilard, R., Eds.; World Scientific Publishing: Singapore, 2010; Vol. *2*, pp 295−367. (b) Harvey, J. D.; Ziegler, C. J. Developments in the Metal Chemistry of N-Confused Porphyrin. *Coord. Chem. Rev.* **2003**, *247*, 1−19.

(14) Muckey, M. A.; Szczepura, L. F.; Ferrence, G. M.; Lash, T. D. Silver(III) Carbaporphyrins: The First Organometallic Complexes of True Carbaporphyrins. *Inorg. Chem.* **2002**, *41*, 4840−4842.

(15) Lash, T. D.; Colby, D. A.; Szczepura, L. F. New Riches in Carbaporphyrin Chemistry: Silver and Gold Organometallic Complexes of Benzocarbaporphyrins. *Inorg. Chem.* **2004**, *43*, 5258−5267.

(16) Sahota, N.; Ferrence, G. M.; Lash, T. D. Synthesis and Properties of Carbaporphyrin and Carbachlorin Dimethyl Esters Derived from Cyclopentanedialdehydes. *J. Org. Chem.* **2017**, *82*, 9715−9730.

(17) Adiraju, V. A. K.; Ferrence, G. M.; Lash, T. D. Rhodium(I), Rhodium(III) and Iridium(III) Carbaporphyrins. *Dalton Trans* **2016**, *45*, 13691−13694.

(18) Lash, T. D.; Ferrence, G. M. Metalation and Selective Oxidation of Diphenyl-23-oxa-, thia-, and Selena-21-carbaporphyrins. *Inorg. Chem.* **2017**, *56*, 11426−11434.

(19) (a) Liu, D.; Lash, T. D. Synthesis, Spectroscopy and Metallation of Mixed Carbaporphyrinoid Systems. *Chem. Commun.*




DOI: 10.1021/acs.organomet.8b00863
*Organometallics* XXXX, XXX, XXX−XXX

**2002**, 2426−2427. (b) Liu, D.; Ferrence, G. M.; Lash, T. D. Oxybenziporphyrins, Oxypyriporphyrins, Benzocarbaporphyrins, and Their 23-Oxa- and 23-Thia-Analogues: Synthesis, Spectroscopic Characterization, Metalation, and Structural Characterization of a Palladium(II) Organometallic Derivative. *J. Org. Chem.* **2004**, *69*, 6079−6093.
(20) Berlicka, A.; Dutka, P.; Szterenberg, L.; Latos-Grazyński, L. Towards True Carbaporphyrinoids: Synthesis of 21-Carba-23-thiaporphyrin. *Angew. Chem., Int. Ed.* **2014**, *53*, 4885−4889.
(21) Lash, T. D. Unexpected Alkyl Group Migration in Palladium(II) Benzocarbaporphyrins. *Org. Lett.* **2011**, *13*, 4632−4635.
(22) Li, D.; Lash, T. D. Synthesis and Reactivity of Carbachlorins and Carbaporphyrins. *J. Org. Chem.* **2014**, *79*, 7112−7121.
(23) Grabowski, E. Y.; AbuSalim, D. I.; Lash, T. D. Naphtho[2,3-*b*]carbaporphyrins. *J. Org. Chem.* **2018**, *83*, 11825−11838.
(24) Szyszko, B.; Latos-Grazyński, L.; Szterenberg, L. A Facile Palladium-Mediated Contraction of Benzene to Cyclopentadiene: Transformations of Palladium(II) *p*-Benziporphyrin. *Angew. Chem., Int. Ed.* **2011**, *50*, 6587−6591.
(25) Pacholska-Dudziak, E.; Skonieczny, J.; Pawlicki, M.; Szterenberg, L.; Ciunik, Z.; Latos- Grazyński, L. Palladium Vacataporphyrin Reveals Conformational Rearrangements Involving Hückel and Möbius Macrocyclic Topologies. *J. Am. Chem. Soc.* **2008**, *130*, 6182−6195.
(26) Yoneda, T.; Saito, S.; Yorimitsu, H.; Osuka, A. Palladium(II)-Triggered Rearrangement of Heptaphyrins to N-Confused Porphyrins. *Angew. Chem., Int. Ed.* **2011**, *50*, 3475−3478.
(27) (a) Lash, T. D. Porphyrin Synthesis by the "3 + 1" Approach: New Applications for an Old Methodology. *Chem. - Eur. J.* **1996**, *2*, 1197−1200. (b) Lash, T. D. What's in a Name? The MacDonald Condensation. *J. Porphyrins Phthalocyanines* **2016**, *20*, 855−888.
(28) Chapelle, J. P.; Elguero, J.; Jacquier, R.; Tarrago, G. Enehydrazines [(alk-1-en-1-yl)hydrazines]. III. Reaction of 1,2-Dimethylhydrazine with Carbonyl Compounds; Formation of *N*-Methylpyrroles and 3-Pyrazolines. *Bull. Soc. Chim. Fr.* **1970**, 3147−3155.
(29) Sessler, J. L.; Johnson, M. R.; Lynch, V. Synthesis and Crystal Structure of a Novel Tripyrrane-containing Porphyrinogen-like Macrocycle. *J. Org. Chem.* **1987**, *52*, 4394−4397.
(30) Boudif, A.; Momenteau, M. A New Convergent Method for Porphyrin Synthesis Based on a '3 + 1' condensation. *J. Chem. Soc., Perkin Trans. 1* **1996**, 1235−1242.
(31) Lash, T. D. Porphyrins with Exocyclic Rings. Part 9. Porphyrin Synthesis by the "3 + 1" Approach. *J. Porphyrins Phthalocyanines* **1997**, *1*, 29−44.
(32) Jackson, A. H.; Pandey, R. K.; Roberts, E. Total Synthesis of an *N*-Methylporphyrin. *J. Chem. Soc., Chem. Commun.* **1985**, 470−471.
(33) Pandey, R. K.; Jackson, A. H.; Smith, K. M. Ring Syntheses of the Four *N*-Methylprotoporphyrin Isomers and of Related *N*-Methyl and *N,N'*-Dimethylporphyrins. *J. Chem. Soc., Perkin Trans. 1* **1991**, 1211−1220.
(34) Arnold, Z. Synthetic Reactions of Dimethylformamide. XXII. Formation and Preparation of Formyl Derivatives of Indene. *Collect. Czech. Chem. Commun.* **1965**, *30*, 2783−2792.
(35) Lash, T. D.; Hayes, M. J.; Spence, J. D.; Muckey, M. A.; Ferrence, G. M.; Szczepura, L. F. Conjugated Macrocycles Related to the Porphyrins. 21. Synthesis, Spectroscopy, Electrochemistry, and Structural Characterization of Carbaporphyrins. *J. Org. Chem.* **2002**, *67*, 4860−4874.
(36) Bruno, I. J.; Cole, J. C.; Kessler, M.; Luo, J.; Motherwell, W. D. S.; Purkis, L. H.; Smith, B. R.; Taylor, R.; Cooper, R. I.; Harris, S. E.; Orpen, A. G. Retrieval of Crystallographically-derived Molecular Geometry Information. *J. Chem. Inf. Comput. Sci.* **2004**, *44*, 2133−2144.
(37) Thompson, S. J.; Brennan, M. R.; Lee, S. Y.; Dong, G. Synthesis and Applications of Rhodium Porphyrin Complexes. *Chem. Soc. Rev.* **2018**, *47*, 929−989.
(38) (a) Brothers, P. J.; Collman, J. P. The Organometallic Chemistry of Transition-Metal Porphyrin Complexes. *Acc. Chem. Res.* **1986**, *19*, 209−215. (b) Wayland, B. B.; Sherry, A. E.; Coffin, V. L. *Homogeneous Transition Metal Catalyzed Reactions*; American Chemical Society: Washington, DC, 2009, Vol. *230*, pp 249−259. (c) Cui, W.; Wayland, B. B. Hydrocarbon C-H Bond Activation by Rhodium Porphyrins. *J. Porphyrins Phthalocyanines* **2004**, *8*, 103−110. (d) de Bruin, B.; Hetterscheid, D. G. H. Paramagnetic (Alkene)Rh and (Alkene)Ir Complexes: Metal or Ligand Radicals? *Eur. J. Inorg. Chem.* **2007**, *2007*, 211−230.
(39) (a) Maxwell, J. L.; O'Malley, S.; Brown, K. C.; Kodadek, T. Shape-selective and Asymmetric Cyclopropanation of Alkenes Catalyzed by Rhodium Porphyrins. *Organometallics* **1992**, *11*, 645−652. (b) O'Malley, S.; Kodadek, T. Asymmetric Cyclopropanation of Alkenes Catalyzed by a Rhodium Chiral Fortress Porphyrin. *Organometallics* **1992**, *11*, 2299−2302. (c) Maxwell, J. L.; Brown, K. C.; Bartley, D. W.; Kodadek, T. Mechanism of the Rhodium Porphyrin-Catalyzed Cyclopropanation of Alkenes. *Science* **1992**, *256*, 1544−1547.
(40) (a) Srinivasan, A.; Toganoh, M.; Niino, T.; Osuka, A.; Furuta, H. Synthesis of N-Confused Tetraphenylporphyrin Rhodium Complexes Having Versatile Metal Oxidation States. *Inorg. Chem.* **2008**, *47*, 11305−11313. (b) Niino, T.; Toganoh, M.; Andrioletti, B.; Furuta, H. Rhodium N-Confused Porphyrin-Catalyzed Alkene Cyclopropanation. *Chem. Commun.* **2006**, *42*, 4335−4337.
(41) Idec, A.; Szterenberg, L.; Latos-Grazyński, L. From *para*-Benziporphyrin to Rhodium(III) 21-Carbaporphyrins: Imprinting Rh···$\eta^2$-CC, Rh···$\eta^2$-CO, and Rh···$\eta^2$-CH Coordination Motifs. *Chem. - Eur. J.* **2015**, *21*, 12481−12487.
(42) Hurej, H.; Pawlicki, M.; Latos-Grazyński, L. Rhodium-Induced Reversible C-C Bond Cleavage: Transformations of Rhodium(III) 22-Alkyl-*m*-benziporphyrins. *Chem. - Eur. J.* **2018**, *24*, 115−126.
(43) (a) Sessler, J. L.; Mozaffari, A.; Johnson, M. R. 3,4-Diethylpyrrole and 2,3,7,8,12,13,17,18-Octaethylporphyrin. *Organic Syntheses*; John Wiley & Sons, Inc.: Hoboken, NJ, 1992; Vol. *70*, p 68. (b) Roth, S. D.; Shkindel, T.; Lightner, D. A. Intermolecularly Hydrogen-bonded Dimeric Helices: Tripyrrindiones. *Tetrahedron* **2007**, *63*, 11030−11039.


DOI: 10.1021/acs.organomet.8b00863
*Organometallics* XXXX, XXX, XXX−XXX